

Analysis of Berkovich Nanoindentation Loading Curves in SiC and SiO₂ Materials

Stefano GUICCIARDI^{*,***,†} and Giuseppe PEZZOTTI^{**,*}

^{*}CNR-ISTEC, Institute of Science and Technology for Ceramics, Via Granarolo 64, I-48018 Faenza, Italy

^{**}Ceramic Physics Laboratory, Kyoto Institute of Technology, Matsugasaki, Sakyo-ku, Kyoto-shi 606-8585

^{***}Research Institute for Nanoscience (RIN), Kyoto Institute of Technology, Matsugasaki, Sakyo-ku, Kyoto-shi 606-8585

On two SiC ceramics and a standard fused silica specimen, depth-sensing indentation tests with a Berkovich indenter were carried out at several peak loads. The loading part of the load–displacement curves were statistically analyzed and it was shown that the loading exponent of the relation $P \propto h^n$ was lower than the expected value of 2 in most of the cases. Factors affecting the loading exponent have been considered and evaluated. It was demonstrated that their effect was minimal on the fitting results.

[Received September 26, 2006; Accepted January 18, 2007]

Key-words : SiC, SiO₂, Nanoindentation, Loading curves, Loading exponent

1. Introduction

Since the fundamental work by Oliver and Pharr,¹⁾ nanoindentation has become a very powerful tool in order to measure mechanical properties, mainly hardness and Young's modulus, in very small volumes of materials or structures. In these tests, an indenter is pressed against a surface and then withdrawn. Both during loading and unloading, the load is registered as a function of the displacement. Simply analyzing this load–displacement curve, properties like hardness, Young's modulus, fracture toughness, film adhesion and residual stresses can be measured.²⁾ By dimensional analysis,³⁾ it can be shown that the load (P) on self-similar indenters, like Berkovich or Vickers, has a square dependence on the displacement (h) during loading if no scale length due to the indented material comes into play, i.e. $P \propto h^2$. However, several papers have reported experimental values of the loading exponent lower than two.^{4)–8)} Many explanations have been proposed to account for this non-perfect square dependence: improper fitting,⁵⁾ tip radius effects,^{6),8),9)} machine compliance,¹⁰⁾ indentation size effects,^{3),9)} material inhomogeneity or fracture.¹¹⁾

In this work, two silicon carbide ceramics with very different grain size and a standard fused silica specimen were tested by Berkovich nanoindentation tests using several peak loads. The loading part of the indentation curves was analyzed to statistically assess the loading exponent n and the influence of the factors which could have impacted on its value. SiC ceramics are an example of polycrystalline hard materials which do not show pile up and are not pressure-sensitive materials like other ceramics.¹²⁾ The very different mean grain size was meant to see if a microstructural scale length is involved in the determination of n . Finally, the silica specimen was added as it is a well-characterized homogeneous isotropic material without microstructure whose hardness and Young's modulus are known to be load-independent.¹³⁾

2. Experimental

The SiC ceramics were sintered by hot-pressing using yttria and alumina as sintering aids. The final densities were > 99% of the theoretical density. By image analysis, the mean grain size was assessed to be (540 ± 10) nm and (78 ± 8) nm, respectively. In the following, the SiC specimens will be labelled according to their mean grain size: S540 and S78. More details on processing and characteristics of the materials are reported

in¹⁴⁾ for sample S540 and in¹⁵⁾ for samples S78. Besides the two SiC ceramics, a standard fused silica specimen was considered. This material is homogeneous, without microstructure and the nanoindentation properties are load-independent.

The depth-sensing indentation tests were performed using a commercial nanoindenter (Nano Indenter XPTM, MTS Systems Corporation, Oak Ridge, TN, USA) with a diamond Berkovich indenter. The main features of this nanoindenter are presented and compared to other commercial and laboratory-made nanoindenters in.¹⁶⁾ The polished SiC and silica specimens were glued to aluminium cylinders. The final surface roughness, R_a , of the specimens were (0.025 ± 0.009) μm , (0.014 ± 0.001) μm and (0.009 ± 0.002) μm for S540, S78 and the silica specimen, respectively. Six peak loads were used to investigate the indentation hardness and Young's modulus as a function of penetration depth: 1, 10, 50, 100, 200 and 400 mN for the silica specimen and 5, 10, 50, 100, 200 and 400 mN for the SiC specimens. The indenter was continuously loaded with prescribed loading rate up to the peak load and immediately unloaded with no holding time. For each peak load, at least ten indentations, spaced at 50 μm , were made. Indentation hardness (H) and Young's modulus (E) were calculated by the data acquisition software of the nanoindenter (TestWorksTM ver. 4.06 A) which is based on the model of Oliver and Pharr,¹⁾ see Fig. 1.

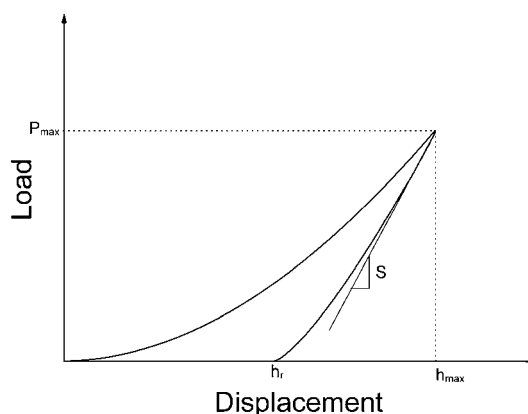


Fig. 1. Typical load vs displacement data for a depth-sensing indentation test. The main parameters are identified: residual displacement (h_r), maximum displacement (h_{max}), maximum load (P_{max}) and unloading contact stiffness (S).

[†] Corresponding author. E-mail address: stefano@istec.cnr.it

$$H = \frac{P_{\max}}{A_c} \quad (1)$$

$$E = \frac{1 - \nu^2}{\frac{1}{E_r} - \frac{1 - \nu_i^2}{E_i}} \quad (2)$$

where P_{\max} is the peak load, A_c the contact area, and E , E_i , ν , ν_i are the Young's modulus and the Poisson ratio of the material and indenter ($E_i = 1141$ GPa and $\nu_i = 0.07$), respectively. E_r , the reduced Young's modulus, is calculated from the unloading data as

$$E_r = \frac{\sqrt{\pi}}{2} S \frac{1}{\beta} \frac{1}{\sqrt{A_c}} \quad (3)$$

where b is a constant equal to 1.034 for a Berkovich indenter and S is the contact stiffness (Fig. 1). The contact stiffness is calculated by fitting a percentage, 90% in our case, of the unloading data by a polynomial function $P = b(h - hf)^m$ and then taking the derivative of this function with respect to the displacement, i.e. dP/dh , and numerically evaluate it at the beginning of the unloading curve. In the O&P model, the contact area, A_c , is defined by a polynomial function $A_c = \sum_{n=0}^8 C_i h_c^{2-n}$ of the contact depth, h_c , which is given by

$$h_c = h_{\max} - \varepsilon \frac{P_{\max}}{S} \quad (4)$$

where h_{\max} is the displacement at the maximum load and ε a constant equal to 0.75. The software of the our nanoindenter automatically subtracted the machine compliance and the thermal drift from the raw loading-unloading data. The area function of the indenter was calibrated on the standard fused silica specimen. The fitting analysis of the loading part of the load-displacement curves was carried out using a commercial mathematical software (MATHEMATICA 5.0, Wolfram Inc., Chicago, IL, USA).

3. Results and discussion

The Young's modulus and the hardness of the tested materials are shown in Fig. 2. For a deeper discussion about these properties in the SiC specimens, the interested reader is addresses to a previous paper.¹⁷⁾ Only the major indications will be resumed here. The Young's modulus of the SiC ceramics was almost load-independent. The good agreement between the Young's modulus of the silica specimen and the reference value of 72 GPa is a first indication of the correct subtraction of the thermal drift and the machine compliance operated by the machine software. The hardness of S540 shows the phenomenon called indentation size effect (ISE) according to which the measured hardness decreases when the peak load is increased,¹⁸⁾ see Fig. 2. The hardness of the nano-sized SiC and the standard silica was instead load-independent.

For all the tests, the loading part of the load-displacement curves were fitted with both models:

$$P = Ah^2 \quad (5)$$

$$P = Ah^n \quad (6)$$

where A is a constant. The goodness of the fitting was evaluated by considering the relative r^2 , i.e. the fraction of the total variance that is explained by the equation.¹⁹⁾ In Fig. 3, the values of r^2 obtained using Eq. (5) are compared to those obtained using Eq. (6). At it can be seen, the latter are always higher than the former, i.e. h^n fitted the loading data better

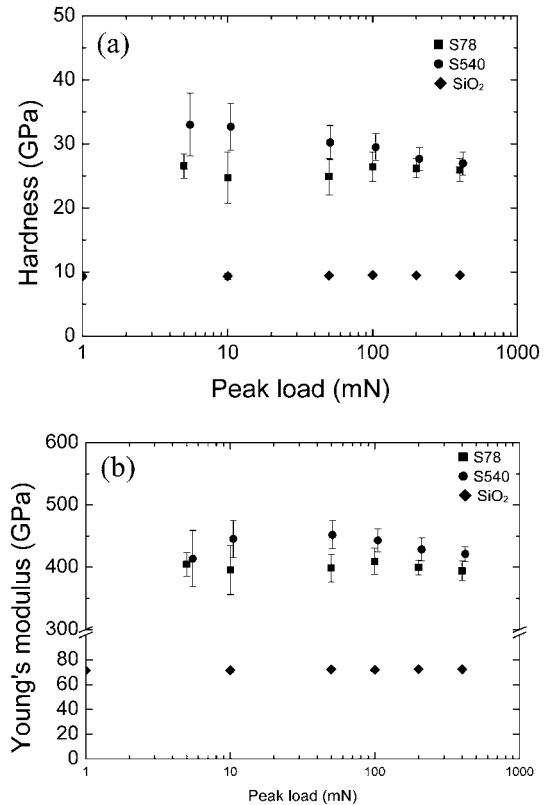


Fig. 2. Hardness (a) and Young's modulus (b) as a function of peak load and material. Points and bars represent mean ± 1 standard deviation, respectively.

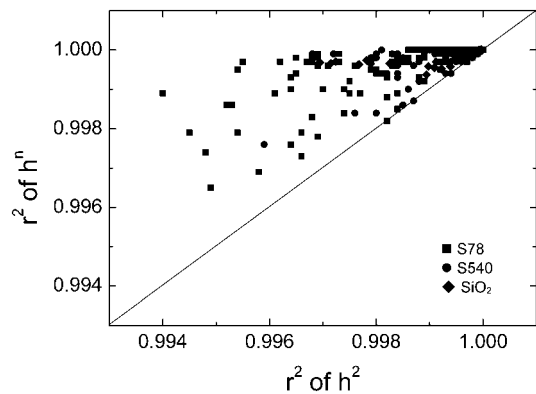


Fig. 3. All-tests comparison of the goodness-of-fit, r^2 , between the models of Eq. (5) on the x-axis and Eq. (6) on the y-axis. The r^2 values relative to Eq. (6) are always better than those relative to Eq. (5) as can be seen from their position above the identity line.

than h^2 . It must be underlined that fitting the loading curve with h^2 furnished very high values of r^2 (> 0.99) in every situation. However, fitting the loading curves with h^n was even better. The results were the same, i.e. $n \neq 2$ was better than $n = 2$, even if the fitting was performed after the transformation of the displacement data as suggested by Hainsworth et al.⁵⁾ According to these authors, the squared dependence was proved in their paper because they showed that a linear fit of the P vs h^2 was better than the linear fit of P vs h^n , where n was the loading exponent obtained by the non-linear fit of the initial load-displacement data. This can be shown to be not

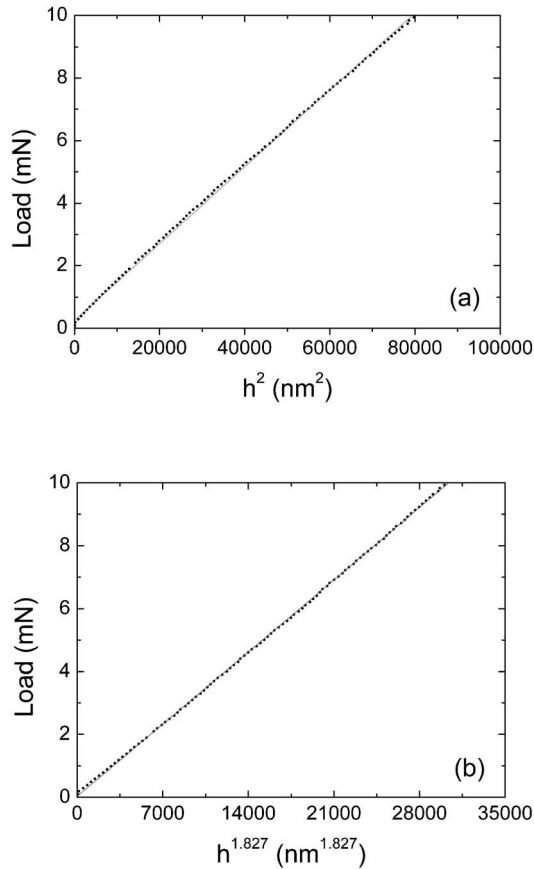


Fig. 4. Linear fit of load (P) vs displacement (h) after displacement transformation: h^2 (a) and h^n (b). The linear fit is better in the second case.

possible by a simple mathematical reasoning. In fact, if a loading exponent n minimizes the sum of squares as a result of the non-linear fitting, the best linear fit of the load and transformed displacement data must be again given by the displacement data elevated to n , and not to a different exponent, since this operation is just a substitution in Eq. (6). In Fig. 4, an example of the same type of those reported by Hainsworth et al.⁵⁾ is shown for a 10 mN test on our silica specimen. As it can be seen, the same exponent which best fitted the loading curve is the same exponent according to which the displacement data should be transformed in order to obtain the best linear fit.

The values of the loading exponent n are shown in Fig. 5 as a function of the peak load and materials. As can be seen, even if there seems to be an asymptotic behaviour, they remain statistically lower than the expected value of 2. Particularly at low peak loads, this difference is rather evident. It must be noted that nor the microstructure nor the mean grain size nor the presence of ISE were discriminating factors as the loading exponent of all the tested materials was always below the theoretical value for all the investigated peak load range.

Especially for the low-loads results, the effects of the tip radius had to be considered. An experimental evaluation of the tip radius was therefore performed. By ultra-low load indentation tests, the tip radius R of the indenter was estimated on totally elastic indentation in the silica specimen. The radius R was evaluated by the hertzian formulation for the elastic contact as:²⁾

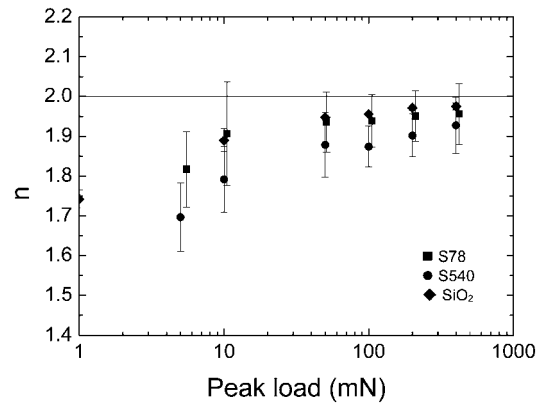


Fig. 5. Loading exponent n as a function of peak load and material. Points and bars represent mean ± 1 standard deviation, respectively. The solid line represents the expected theoretical value of 2.

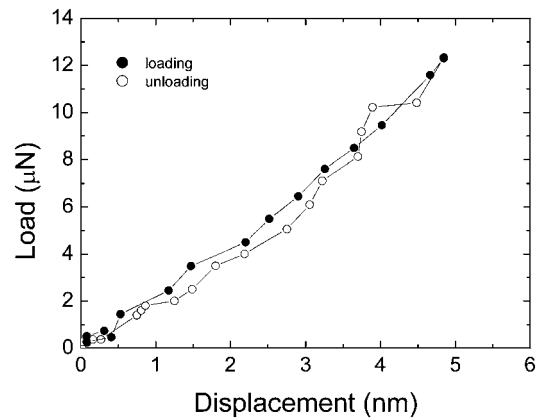


Fig. 6. Totally elastic response of ultra-low load indentation in the standard fused silica specimen.

$$P = \frac{4}{3} E_r R^{1/2} h^{3/2}. \quad (7)$$

An example of a totally elastic response of the fused silica at low load is shown in Fig. 6. The tip radius R of our Berkovich indenter was estimated to be (152 ± 28) nm. As reported by Giannakopoulos and Suresh,²⁰⁾ the effect of the tip radius disappears when the penetration h is $> R/40$. For the same situation, Cheng and Cheng²¹⁾ indicated that h/R should be ≥ 0.073 . All the penetrations involved in this study well satisfy both the requirements, see Fig. 7, so that the tip radius was not a reason for n to be lower than 2.

Another factor which could make n different from 2 has been indicated in the machine compliance.¹⁰⁾ We will therefore analyze how well the machine compliance was subtracted from our raw data. To do this, one can see that if the hardness and the Young's modulus of a material are load-independent, then from Eqs. (1) and (3) one obtains

$$C = b \frac{1}{\sqrt{P_{\max}}} \quad (8)$$

where C is $1/S$ and b is a constant given by $\sqrt{\pi}/2\beta \sqrt{H}/E_r$.²²⁾ Therefore, by fitting with Eq. (8) the experimental total compliance versus the inverse of the square root of the peak load, the resulting fitting equation should have an intercept statistically equal to zero. A non-zero intercept implies that

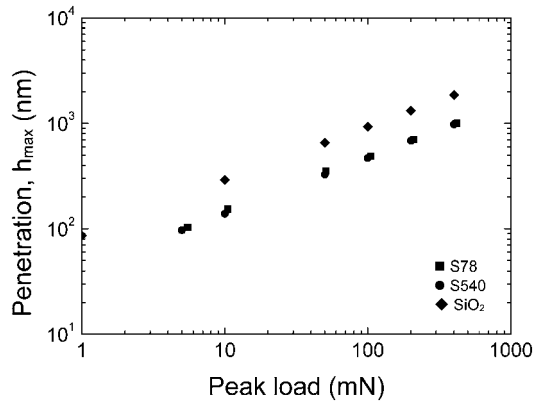


Fig. 7. Maximum penetration, h_{\max} , as a function of peak load and material. Points and bars represent mean ± 1 standard deviation, respectively.

the machine compliance is not correctly subtracted from the raw load–displacement data or that the hardness or the Young’s modulus of the material are load-dependent. For the tested materials, the plots of the experimental data along with the respective fitting curves are shown in Fig. 8. As it can be seen, for materials with no ISE, i.e. the nano-sized SiC and the fused silica, the fitting curves pass through the axes origin. In the case of S540, the value of the intercept was statistically different from 0 but this was due to its marked ISE, see Figs. 8 (b) and 2(a).

The last issues which could have affected the loading exponent are material inhomogeneity or fracture. About the former, even if it could hold for the SiC specimens it is out of question for the silica specimen as this is a homogeneous material without microstructure, at least at the indentation depths involved in this study. It is in fact known that the surface chemistry of silica and SiC ceramics shows a different composition than the bulk chemistry: hydrated in the former²³⁾ and oxidized in the latter.²⁴⁾ However, the loading exponent is lower than 2 even at high penetration depths when the surface chemistry effects can be safely ignored. If fracture is considered, we have shown that the loading exponent is lower than 2 both at low loads, when cracks are very unlikely to be present, and at high loads, where fracture can characterize the indentation marks. However, the cracking threshold in ceramics materials has been reported to be about 250 mN.²⁵⁾ This means that most of our indentations were crack-free.

At the moment, it is not clear why the experimental loading exponent was statistically lower than 2. The possible explanation could be rooted in factors never considered before.

4. Conclusions

Two SiC ceramics and a standard fused silica specimen have been characterized by nanoindentation tests using several peak loads. The loading part of the load-displacement data was statistically analyzed. It was shown that the fitting were always better with a loading exponent n lower than the theoretical value of 2. The factors which could affect the value of the loading exponent were considered: mode of fitting, tip radius, machine compliance, materials inhomogeneity or fracture. It was demonstrated that the effect of these factors was negligible. At the moment, no clear explanation can be provided for the difference with the expected square dependence of the load with the displacement.

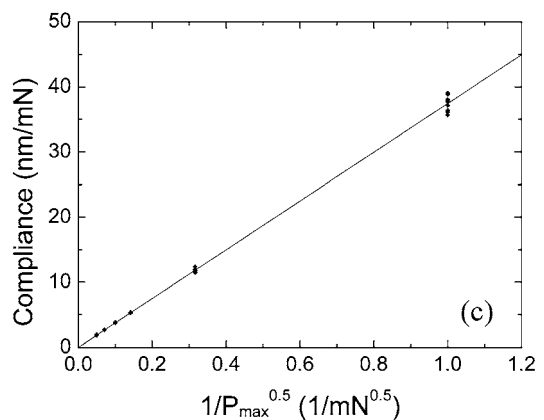
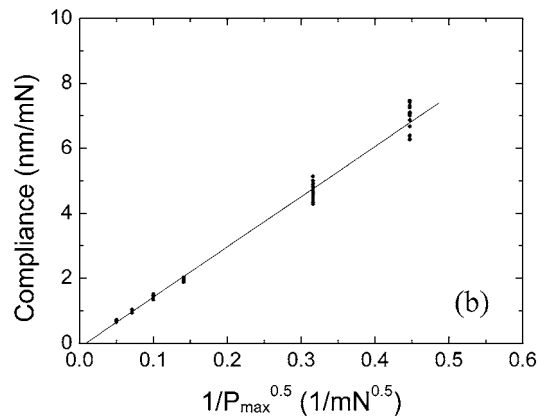
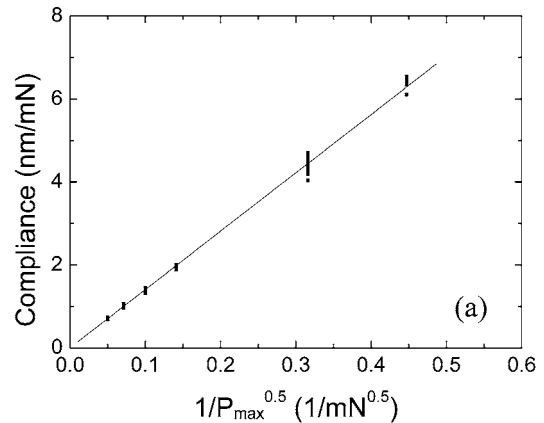


Fig. 8. Linear fitting of the total compliance, C , vs $(P_{\max})^{-0.5}$. The fitting lines pass through the origin of the axes for S78 (a) and the fused silica (c) which means that the machine compliance was correctly subtracted. In case of S540 (b), the fitting line has a negative intercept. This was due to its marked indentation size effect.

References

- 1) Oliver, W. C. and Pharr, G. M., *J. Mater. Res.*, Vol. 7, pp. 1564–1583 (1992).
- 2) Fisher-Cripps, A. C., *Nanoindentation*, 2nd ed., Springer-Verlag, New York (2004).
- 3) Cheng, Y.-T. and Cheng, C.-M., *Mater. Sci. Eng. Rep.*, Vol. 44, pp. 91–149 (2004).
- 4) Loubet, J. L., Georges, J. M. and Meille, G., *Microindentation Techniques in Materials Science and Engineering*, ASTM STP 889, Blau, P. J. and Lawn, B. R., Eds., American Society for Testing and Materials, Philadelphia (1986) pp. 72–89.
- 5) Hainsworth, S. V., Chandler, H. W. and Page, T. F., *J. Mater. Res.*, Vol. 11, pp. 1987–1995 (1996).

- 6) Gerberich, W. W., Yu, W., Kramer, D., Strojny, A., Bahr, D., Lilleoden, E. and Nelson, J., *J. Mater. Res.*, Vol. 13, pp. 421–439 (1998).
- 7) Lim, Y. Y., Chaudhri, M. M. and Enomoto, Y., *J. Mater. Res.*, Vol. 14, pp. 2314–2327 (1999).
- 8) Zeng, K. and Chiu, C.-h., *Acta Mater.*, Vol. 49, pp. 3539–3551 (2001).
- 9) Pharr, G. M. and Bolshakov, A., *J. Mater. Res.*, Vol. 17, pp. 2660–2671 (2002).
- 10) Sakai, M., Shimizu, S. and Ishikawa, T., *J. Mater. Res.*, Vol. 14, pp. 1471–1484 (1999).
- 11) Cheng, Y.-T., Li, Z. and Cheng, C.-M., *Phil. Mag.*, Vol. 82, pp. 1821–1829 (2002).
- 12) Giannakopoulos, A. E. and Larsson, P.-L., *Mechanics of Mater.*, Vol. 25, pp. 1–35 (1997).
- 13) Nix, W. D., *Mater. Sci. Eng.*, Vol. A234–236, pp. 37–44 (1997).
- 14) Sciti, D. and Bellosi, A., *J. Mater. Sci.*, Vol. 35, pp. 3849–3855 (2000).
- 15) Sciti, D., Vicens, J., Herlin, N., Grabis, J. and Bellosi, A., *J. Ceram. Proc. Res.*, Vol. 5, pp. 40–47 (2004).
- 16) Sawa, T. and Tanaka, K., *J. Mater. Res.*, Vol. 16, pp. 3084–3096 (2001).
- 17) Guicciardi, S., Sciti, D., Melandri, C. and Bellosi, A., *J. Am. Ceram. Soc.*, Vol. 87, pp. 2101–2107 (2004).
- 18) McColm, I. J., “Ceramic Hardness,” Plenum Press, New York (1990).
- 19) Beck, J. V. and Arnold, K. J., “Parameter Estimation in Engineering and Science,” John Wiley & Sons, New York (1977).
- 20) Giannakopoulos, A. E. and Suresh, S., *Scripta Mater.*, Vol. 40, pp. 1191–1198 (1999).
- 21) Cheng, Y.-T. and Cheng, C.-M., *J. Mater. Res.*, Vol. 13, pp. 1059–1064 (1998).
- 22) Troyon, M. and Huang, L., *J. Mater. Res.*, Vol. 20, pp. 610–617 (2005).
- 23) Doremus, R. H., *J. Mater. Res.*, Vol. 10, pp. 2379–2389 (1995).
- 24) Amy, F., Enriquez, H., Soukiassian, P., Storino, P.-F., Chabal, Y. J., Mayne, A. J., Dujardin, G., Hwu, Y. K. and Brylinski, C., *Phys. Rev. Lett.*, Vol. 86, pp. 4342–4345 (2003).
- 25) Jayaraman, S., Hahn, G. T., Oliver, W. C., Rubin, C. A. and Bastias, P. C., *Int. J. Solids Struct.*, Vol. 35, pp. 365–381 (1998).